A New Simple Model for Land Mobile Satellite Channels: First- and Second-Order Statistics

Ali Abdi, Wing C. Lau, Mohamed-Slim Alouini, and Mostafa Kaveh

Abstract __ In this paper we propose a new shadowed Rice model for land mobile satellite channels. In this model, the amplitude of the line-of-sight is characterized by the Nakagami distribution. The major advantage of the model is that it leads to closed-form and mathematically-tractable expressions for the fundamental channel statistics such as the envelope probability density function, moment generating function of the instantaneous power, and the level crossing rate. The model is very convenient for analytical and numerical performance prediction of complicated narrowband and wideband land mobile satellite systems, with different types of uncoded/coded modulations, with or without diversity. Comparison of the first- and the second-order statistics of the proposed model with different sets of published channel data demonstrates the flexibility of the new model in characterizing a variety of channel conditions and propagation mechanisms over satellite links. Interestingly, the proposed model provides a similar fit to the experimental data as the well-accepted Loo's model, but with significantly less computational burden.

Keywords: Satellite channels, Land mobile satellite systems, Channel modeling, Nakagami model, Rice model, Loo's model, Shadowed Rice model, Level crossing rate, Average fade duration, Performance evaluation, Diversity, Interference.

Paper category: Propagation and channel characterization.

Corresponding author: Ali Abdi
Dept. of Electrical and Computer Engineering
New Jersey Institute of Technology
323 King Blvd.
Newark, NJ 07102, USA

Phone: (973) 596 5621
Fax: (973) 596 5680
Email: ali.abdi@njit.edu

I. INTRODUCTION

Land mobile satellite (LMS) systems are an important part of the third and fourth generation of wireless systems. The significance of such systems is rapidly growing for a variety of applications such as navigation, communications, broadcasting, etc. LMS systems provide services which are not feasible via land mobile terrestrial (LMT) systems. As a complement to LMT systems, LMS systems are able to serve many users over a wide area with low cost. For extensive surveys on different aspects of LMS systems and services, the reader may refer to [1] [2].

The quality of service provided by LMS systems strongly depends on the propagation channel between the satellite and the mobile user. As such, an accurate statistical model for the LMS channel is required for calculating fade margins, assessing the average performance of modulation and coding schemes, analyzing the efficiency of communication protocols, and so on. Similar to the LMT channels, a simple yet efficient model for wideband LMS channels is the tapped delay line model [3] [4], where each tap is described by a narrowband model. Hence, in this paper, we mainly focus on narrowband models, which are the basic building blocks of wideband models.

Generally speaking, the available statistical models for narrowband LMS channels can be placed into two categories: *single* models and *mixture* models. In a single model, the channel is characterized by a single statistical distribution, while a mixture model refers to a combination (weighted summation) of several statistical distributions. Single models are valid for stationary conditions, where the channel statistics remain approximately constant over the time period of interest in a small area. On the other hand, the mixture models are developed for nonstationary channels, where the signal statistics vary significantly over the observation interval in large areas. In Table I and Table II, a list of the proposed single and mixture models for narrowband LMS channels are given, respectively. To understand the details of the single models of Table I, we need to provide a brief overview of the mechanism of random fading in LMS channels.

The random fluctuations of the signal envelope in a narrowband LMS channel can be attributed to two types of fading: multipath fading and shadow fading [5]. We further divide the shadow fading into the line-of-sight (LOS) shadow fading and multiplicative shadow fading. Notice that the multipath components consist of a LOS component and many weak scatter components. In an ideal LMS channel without any type of fading, where there is a clear LOS between the satellite and the land user, without any obstacle in between, hence, no scatter component, the envelope is a non-random constant (at a given instant of time). Due to multipath fading, caused by the weak scatter components propagated via different non-LOS paths, together with the nonblocked LOS component, the envelope becomes a Rice random variable. LOS shadow fading comes from the complete or partial blockage of the LOS by buildings, trees, hills, mountains, etc., which in turn makes the amplitude of the LOS component a random variable. On the other hand, multiplicative shadow fading refers to the random variations of the total power of the multipath components, both the LOS and scatter components. These definitions clearly describe the statistical structures of the single models in Table I. Notice that the structures of the models of [8] and [9] are slightly different from the others in Table I. The first model generalizes the model of Corazza and Vatalaro [7] by including an extra additive scatter component, while the second model extends Loo's model of [6] by assuming that the power of the scatter components in Loo's model is a lognormal variable, independent of the LOS component. The first-order statistics of Loo's model and the model of Corazza and Vatalaro, i.e., the PDF and the cumulative distribution function (CDF) of the envelope, are discussed in [6] and [7], respectively. For the second-order statistics, the level crossing rate (LCR) and the average fade duration (AFD) of the envelope, we refer the readers to [13] and [14], respectively. Notice that the second-order statistics of Loo's model and the model of Corazza and Vatalaro, given in [6] and [15], respectively, are approximate results. In [8], [9], [11], and [12], only the first-order statistics of the models are discussed, while in [10], just the second-order statistics are studied.

Each mixture model in Table II is composed of at least two distributions, where each distribution corresponds to a particular stationary channel state. The models of [16], [17], and [21] have two distributions, while those of [18], [19], and [20] consist of three distributions.

Now let us define a shadowed Rice model as a Rice model in which the LOS is random. Among the proposed models for LMS channels, the shadowed Rice model proposed originally by Loo [6] has found wide applications in different frequency bands such as the UHF-band [24], L-band [22] [24], S-band [23], and Ka-band [24]. In Loo's model, the amplitude of the LOS component is assumed to be a lognormal random variable. However, as discussed in [25], the application of the lognormal distribution for characterizing shadow fading most often results in complicated expressions for the key first and second-order channel statistics such as the envelope PDF and the envelope LCR, respectively. Analytic manipulation of those expressions is usually hard, as they cannot be written in terms of known mathematical functions. This, in turn, makes data fitting and parameter estimation for the lognormal-based models a complex and time-consuming task. Performance evaluation of communication systems such as interference analysis or calculation of the average bit error rate (BER) for single and multichannel reception, is even much more difficult for the lognormal-based models, as sometimes even the numerical procedures for these models fail to give the correct answer.

On the other hand, as conjectured in [25], application of the gamma distribution, as an alternative to the lognormal distribution, can result in simpler statistical models with the same performance for practical cases of interest. In this paper, we assume the power of the LOS component is a gamma random variable. Since the square root of a gamma variable has Nakagami distribution [26], this means that we are modeling the amplitude of the LOS component with a Nakagami distribution. As we will see in the sequel, a Rice model with Nakagami-distributed LOS amplitude constitutes a versatile model which not only agrees very well with measured LMS channel data, but also offers significant analytical and numerical advantages for system performance predictions, design issues, etc.

The rest of this paper is organized as follows. In Section II the first-order statistics of the proposed model, such as the envelope PDF, moments, and the moment generating function (MGF) of the instantaneous power are derived. A connection between the parameters of Loo's model and our model is also established. Section III is devoted to the derivation of second-order statistics of the proposed model, i.e., the LCR and AFD. In Section IV, the first- and the second-order statistics of the proposed model are compared with published measured data. Finally, the paper concludes with a summary given in Section V.

II. FIRST-ORDER STATISTICS OF THE NEW MODEL

According to the definition of the scatter and LOS components provided earlier, the lowpass-equivalent complex envelope of the stationary narrowband shadowed Rice single model can be written as $\Re(t) = A(t)\exp[j\alpha(t)] + Z(t)\exp(j\zeta_0)$, $j^2 = -1$, where $\alpha(t)$ is the stationary random phase process with uniform distribution over $[0, 2\pi)$, while ζ_0 is the deterministic phase of the LOS component. The independent stationary random processes $A(t)$ and $Z(t)$, which are also independent of $\alpha(t)$, are the amplitudes of the scatter and the LOS components, following Rayleigh and Nakagami distributions, respectively

$$p_A(a) = \frac{a}{b_0}\exp\left(\frac{-a^2}{2b_0}\right), \quad a \geq 0,$$
$$p_Z(z) = \frac{2m^m}{\Gamma(m)\ \ \Omega^m} z^{2m-1}\exp\left(\frac{-m z^2}{\Omega}\right), \quad z \geq 0, \tag{1}$$

where $2b_0 = E[A^2]$ is the average power of the scatter component, $\Gamma(.)$ is the gamma function, $m = \left(E[Z^2]\right)^2 \big/ Var[Z^2] \geq 0$ is the Nakagami parameter with $Var[.]$ as the variance, and $\Omega = E[Z^2]$ is the average power of the LOS component. The reader should notice that in the traditional Nakagami model for multipath fading [26], *m* changes over the limited range of $m \geq 0.5$, while here we allow *m* to vary over the wider range of $m \geq 0$. This enables the Nakagami PDF to model different types of LOS conditions in a variety of LMS channels [5]. For $m = 0$ we have $p_Z(z) = \delta(z)$, with $\delta(.)$ as the Dirac delta function, which corresponds to urban areas with complete obstruction of the LOS. The case of $0 < m < \infty$ is associated with suburban and rural areas with partial obstruction of the LOS. For $m = \infty$ we have $p_Z(z) = \delta(z - \sqrt{\Omega})$, which corresponds to open areas with no obstruction of the LOS. Of course the extreme cases of $m = 0$ and $m = \infty$ cannot be met in practice, and in real-world situations we expect nonzero small and finite but large values of *m* for urban and open areas, respectively. The moderate values of *m* corresponds to suburban and rural areas.

Let us define the envelope as $R(t) = |\Re(t)|$. Using the same notation as [6], the shadowed Rice PDF for the signal envelope in an LMS channel can be written as

$$p_R(r) = E_Z\left[\frac{r}{b_0}\exp\left(-\frac{r^2 + Z^2}{2b_0}\right) I_0\left(\frac{Z\,r}{b_0}\right)\right], \quad r \geq 0, \tag{2}$$

where $E_Z[.]$ is the expectation with respect to *Z* and $I_n(.)$ is the *n*th-order modified Bessel function of the first kind. Notice that conditioned on *Z*, the argument of the expectation in (2) is nothing but the Rice PDF. By calculating the expectation of (2) with respect to the Nakagami distribution of (1) using [27], and after some algebraic manipulations, we obtain the new envelope PDF

$$p_R(r) = \left(\frac{2b_0 m}{2b_0 m + \Omega}\right)^m \frac{r}{b_0}\exp\left(-\frac{r^2}{2b_0}\right) {}_1F_1\left(m, 1, \frac{\Omega\, r^2}{2b_0(2b_0 m + \Omega)}\right), \quad r \geq 0, \tag{3}$$

where ${}_1F_1(.,.,.)$ is the confluent hypergeometric function [28]. For $m = 0$, Eq. (3) simplifies to the Rayleigh PDF in (1), i.e., $\left(r/b_0\right)\exp\left(-r^2/2b_0\right)$, while for $m = \infty$ it reduces to the Rice PDF $\left(r/b_0\right)\exp\left(-(r^2 + \Omega)/2b_0\right) I_0\left(\sqrt{\Omega}\ r/b_0\right)$. On the other hand, in Loo's model [6], the LOS amplitude is assumed to follow the lognormal distribution

$$p_Z(z) = \frac{1}{\sqrt{2\pi d_0}\, z} \exp\left[-\frac{(\ln z - \mu)^2}{2 d_0} \right], \quad z \geq 0, \tag{4}$$

where $\mu = E[\ln Z]$ and $d_0 = Var[\ln Z]$. In contrast with Loo's PDF, which includes an infinite-range integral, the new PDF has a compact form in terms of the tabulated function ${}_1F_1(.,.,.)$, also available in standard mathematical packages such as Mathematica©, for both numerical and symbolic operations. The interested reader may refer to [29] for more details on the numerical computation of ${}_1F_1(.,.,.)$. Using [27], the moments of the proposed PDF can be shown to be

$$E[R^k] = \left(\frac{2b_0 m}{2b_0 m + \Omega} \right)^m (2b_0)^{\frac{k}{2}} \; \Gamma\left(\frac{k}{2} + 1 \right) {}_2F_1\left(\frac{k}{2} + 1, \; m, \; 1, \; \frac{\Omega}{2b_0 m + \Omega} \right), \quad k = 0, \; 1, \; 2, \; \ldots, \tag{5}$$

where ${}_2F_1(.,.,.,.)$ is the Gauss hypergeometric function [28], also available in Mathematica©.

By definition, $S(t) = R^2(t)$ is the instantaneous power, and its PDF can be derived from (3) as[1]

$$p_S(s) = \left(\frac{2b_0 m}{2b_0 m + \Omega} \right)^m \frac{1}{2b_0} \exp\left(-\frac{s}{2b_0} \right) {}_1F_1\left(m, 1, \frac{\Omega s}{2b_0 (2b_0 m + \Omega)} \right), \quad s \geq 0. \tag{6}$$

As demonstrated in [34], the moment generating function (MGF) of the instantaneous power, defined by $M_S(\eta) = E[\exp(-\eta S)]$, $\eta \geq 0$, plays a key role in calculating the BER and the symbol error rate (SER) of different modulation schemes over fading channels. In our model, the MGF of *S*, with the help of [27], can be shown to be

$$M_S(\eta) = \frac{(2b_0 m)^m (1 + 2b_0 \eta)^{m-1}}{\left[(2b_0 m + \Omega)(1 + 2b_0 \eta) - \Omega \right]^m}, \quad \eta \geq 0. \tag{7}$$

The simple mathematical form of the above MGF in the new model entails straightforward performance evaluation procedures for several modulation schemes of interest (with and without diversity reception). On the other hand, the MGF of *S* in Loo's model can be expressed at most in terms of an infinite-range integral or a double infinite sum [35]. Since the numerical manipulation of both representations of Loo's

---

[1] At the time of writing this paper, we discovered that the PDF in (6) is also used for the analysis of radar signals [30]. Some extensions of (6) are discussed in [31] and [32], in the contexts of radar and noise theory, respectively. In the area of statistical distribution theory, a natural generalization of (6) is given in [33].

MGF is time consuming, several approximate expressions are proposed for different cases [35].

Before concluding this section, we establish a useful connection between the parameters of the new model and Loo's model. With v as a positive real number, it is easy to show that $\ln E[Z^v]$ for Nakagami and lognormal PDFs in (1) and (4) can be written as

$$\ln E[Z^v] = \frac{1}{2}\left[\ln\left(\frac{\Omega}{m}\right) + \Psi(m)\right]v + \frac{\Psi'(m)}{8}v^2 + \frac{\Psi''(m)}{48}v^3 + \frac{\Psi'''(m)}{384}v^4 + \ldots, \tag{8}$$

$$\ln E[Z^v] = \mu\, v + \frac{d_0}{2}v^2, \tag{9}$$

where $\Psi(.)$, $\Psi'(.)$, $\Psi''(.)$, and $\Psi'''(.)$ are the psi function and its derivatives, respectively [28]. The absolute values of the psi function and its derivatives converge to zero very fast, as m increases. By second-order matching of the two expressions in (8) and (9), the following relationship between the two sets of parameters (m,Ω) and (μ, d_0) can be established

$$\mu = \frac{1}{2}\left[\ln\left(\frac{\Omega}{m}\right) + \Psi(m)\right], \tag{10}$$

$$d_0 = \frac{\Psi'(m)}{4}. \tag{11}$$

For a given d_0, the corresponding m can be easily obtained by solving the equation in (11), numerically. The value of Ω can be calculated by inverting the equation in (10), which yields $\Omega = m \exp\left[2\mu - \Psi(m)\right]$.

As we will see later, Loo's distribution and our distribution closely match, if one computes our parameter set (b_0, m, Ω) from the Loo's parameter set $(b_0,\ \mu,\ d_0)$, using the relations in (10) and (11).[2] This is particularly useful when we wish to apply the new model with unknown parameters to a set of data collected previously, but the measured data is not available for parameter estimation, or we may not want to go through the time-consuming procedures of parameter estimation. In these cases, the parameters of our model can be obtained from the estimated Loo's parameters, using (10) and (11).

III. SECOND-ORDER STATISTICS OF THE NEW MODEL

The envelope LCR, which is the rate at which the envelope crosses a certain threshold, and the

[2] Notice that b_0 is the same in both models.

envelope AFD, which is the length of the time that the envelope stays below a given threshold, are two important second-order statistics of fading channels, which, for example, carry useful information about the burst error statistics [36]. Therefore, for different system engineering issues such as choosing the frame length for coded packetized systems, designing interleaved or non-interleaved concatenated coding methods [36], optimizing the interleaver size, choosing the buffer depth for adaptive modulation schemes [37], and throughput estimation of communication protocols [38], we need to calculate the envelope LCR and AFD of the fading model of interest. In particular, the LCR and AFD calculation techniques should also work for diversity systems, which have proven to be useful in combating the deleterious effects of fading. In what follows, we develop a characteristic function (CF)-based formula [39] for the envelope LCR of our shadowed Rice model, as the traditional PDF-based approach seems to be intractable, particularly for multichannel reception.

Let us define the envelope LCR, $N_R(r_{th})$, as the average number of times that $R(t)$ crosses the given threshold r_{th} with negative slope, per unit time. For mathematical convenience, we first derive an expression for $N_S(s_{th})$, with s_{th} as the instantaneous power threshold. The envelope LCR can be easily obtained according to $N_R(r_{th}) = N_S(r_{th}^2)$.

It is shown in [39] that the LCR of $S(t)$, corresponding to the threshold s_{th}, can be obtained by

$$N_S(s_{th}) = \frac{-1}{4\pi^2} \int_{-\infty}^{\infty} \int_{-\infty}^{\infty} \frac{1}{\omega_2} \frac{d}{d\omega_2} \Phi_{S\dot{S}}(\omega_1, \omega_2) \exp(-j\omega_1 s_{th})\, d\omega_1 d\omega_2 \,, \tag{12}$$

where $\dot{S}(t)$ is the time derivative of $S(t)$, and $\Phi_{S\dot{S}}(\omega_1, \omega_2)$ is the joint CF of S and $\dot{S}$, defined by $E[\exp(j\omega_1 S + j\omega_2 \dot{S})]$. It is shown in the Appendix that for our proposed model, the joint CF can be found in the following closed-form expression

$$\Phi_{S\dot{S}}(\omega_1, \omega_2) = m^{m+\frac{1}{2}} \vartheta^{m-\frac{1}{2}} (\chi \Omega\, b_0\, \omega_2^2 + m\vartheta)^{-\frac{1}{2}} \left[\left\{ 2b_2 + \frac{\chi\, \Omega}{2(\chi \Omega\, b_0\, \omega_2^2 + m\vartheta)} \right\} \Omega\, \omega_2^2 - j\,\omega_1\, \Omega + m\vartheta \right]^{-m} , \tag{13}$$

in which $\vartheta = 1 + 4(b_0 b_2 - b_1^2)\omega_2^2 - j2b_0\omega_1$. The parameter b_n, $n = 0,1,2$, is the nth spectral moment of the scatter component of the complex envelope $\Re(t)$, defined by $b_n = j^{-n} C_{\Re}^{(n)}(0)$, where $C_{\Re}(\tau) = \frac{1}{2} E[\Re^*(t)\Re(t+\tau)] - \frac{1}{2} \left| E[\Re(t)] \right|^2$ is the autocovariance of $\Re(t)$. The parameter χ in (13) is the average power of the time derivative of $I(t) = Z^2(t)$, defined by $\chi = -D_I''(0) = E[\dot{I}^2(t)]$ [40], where $D_I(\tau) = \left\{ E[I(t)I(t+\tau)] - (E[I(t)])^2 \right\} \big/ \left\{ E[I^2(t)] - (E[I(t)])^2 \right\}$ is the normalized autocovariance of $I(t)$ and prime represents differentiation with respect to τ. As expected, $\Phi_{S\dot{S}}(j\eta, 0)$ in (13) matches the

MGF $M_S(\eta)$ given in (7), while as $\chi \to 0$ and $m \to \infty$ (time-invariant non-random LOS with amplitude $\sqrt{\Omega}$), $\Phi_{S\dot{S}}(\omega_1,\omega_2)$ in (13) converges to the corresponding result for the Rice fading model, given in [39], i.e., $\vartheta^{-1}\exp[-\Omega(2b_2\omega_2^2 - j\omega_1)/\vartheta]$. By substituting (13) into (12), $N_S(s_{th})$ and consequently $N_R(r_{th})$ can be calculated numerically, using a standard mathematical package such as Mathematica©. Notice that the bivariate CF $\Phi_{S\dot{S}}(\omega_1,\omega_2)$ in (13) plays the same role as the univariate MGF $M_S(\eta)$ in (7), as it allows straightforward LCR calculation in diversity systems.

So far, we have calculated the LCR of the new LMS model for the general case in which the maximum Doppler frequency of the LOS component, $f_{\max}^{\text{LOS}}$, which is the bandwidth of $Z(t)$, is not negligible. However, empirical observations have shown that the rate of change of the LOS component (several Hz) is significantly less than that of the scatter component (several hundred Hz) [22]. In other words, $f_{\max}^{\text{LOS}} / f_{\max}^{\text{scatter}} \ll 1$, where $f_{\max}^{\text{scatter}}$ is the maximum Doppler frequency of the scatter component. Roughly speaking, this implies that $\dot{Z}(t) \approx 0$, i.e., over the observation interval we have $Z(t) \equiv Z$, a random variable and not a random process. Under this condition we have $\chi = 0$, which simplifies (13) drastically to

$$\Phi_{S\dot{S}}(\omega_1,\omega_2) = m^m \vartheta^{m-1}\left(2b_2\Omega\,\omega_2^2 - j\,\omega_1\,\Omega + m\,\vartheta\right)^{-m}. \tag{14}$$

On the other hand, under the assumption of $f_{\max}^{\text{LOS}} / f_{\max}^{\text{scatter}} \ll 1$, it is possible to proceed with the PDF-based approach and derive a closed-from solution for the LCR of the new model. In fact, by averaging Eqs. (4.13) and (4.14) in [41] with respect to the Nakagami-distributed LOS amplitude we obtain

$$N_R(r_{th}) = \frac{1}{\sqrt{2\pi}\,\Gamma(m)}\left(\frac{2b_0 m}{2b_0 m + \Omega}\right)^m \sqrt{\frac{b_0 b_2 - b_1^2}{b_0}}\,\frac{r_{th}}{b_0}\exp\left(-\frac{r_{th}^2}{2b_0}\right)\sum_{n=0}^{\infty}\frac{\left(\frac{1}{2}\right)_n(-1)^n}{n!}\left[\xi_n(r_{th}) + \xi_{n+1}(r_{th})\right], \tag{15}$$

where $(x)_n = x(x+1)\cdots(x+n-1)$, $(x)_0 = 1$, and

$$\xi_n(r_{th}) = \frac{\Gamma(n+m)}{2^n n!}\left[\frac{b_1^2}{b_0(b_0 b_2 - b_1^2)}\right]^n \left(\frac{2b_0\Omega}{2b_0 m + \Omega}\right)^n {}_1F_1\left(n+m, n+1, \frac{\Omega\, r_{th}^2}{2b_0(2b_0 m + \Omega)}\right). \tag{16}$$

With $\chi = 0$, the numerical results of (12) and (15) are exactly the same, as expected. Nevertheless, (12) can be easily applied to diversity systems, while (15) only holds for single antenna receivers and its extension to diversity receivers seems to be intractable.

The CF-based approach for the LCR of Loo's model is not so convenient, as $\Phi_{S\dot{S}}(\omega_1,\omega_2)$ in Loo's model takes an integral form, much more complicated than the closed-form expression of our model in

(13). For a slowly varying LOS, the following result is derived in [13] for Loo's LCR, using the PDF-based approach

$$N_R(r_{th}) = \frac{\sqrt{\beta}\, r_{th}}{\pi^2 b_0 \sqrt{d_0}} \exp\left(-\frac{r_{th}^2}{2b_0}\right) \int_0^\infty \frac{1}{z} \exp\left[-\frac{(\ln z - \mu)^2}{2d_0}\right] \exp\left(-\frac{z^2}{2b_0}\right)$$
$$\int_0^{\pi/2} \cosh\left(\frac{r_{th}\, z \cos x}{b_0}\right) \left\{\exp[-(\varepsilon z \sin x)^2] + \sqrt{\pi}\, \varepsilon z \sin(x) \operatorname{erf}(\varepsilon z \sin x)\right\} dx\, dz, \quad (17)$$

where cosh(.) is the hyperbolic cosine, $\operatorname{erf}(y) = \left(2/\sqrt{\pi}\right) \int_0^y \exp(-x^2) dx$ is the error function, and

$$\beta = b_2 - \left(b_1^2 / b_0\right), \quad \varepsilon = -b_1 \Big/ \left(b_0 \sqrt{2\beta}\right). \quad (18)$$

For any fading model, the envelope AFD, $T_R(r_{th})$, is the average time period over which $R(t)$ stays below a given threshold r_{th}, per unit time. Hence $T_R(r_{th}) = \int_0^{r_{th}} p_R(r) dr \Big/ N_R(r_{th})$, where $p_R(r)$ for the new model is given in (3).

IV. COMPARISON WITH PUBLISHED MEASUREMENTS

A. First-order statistics

First we consider two sets of published Loo's parameters $(b_0,\ \mu,\ d_0)$ [6] [42], estimated from data collected in Canada. These parameter values are listed in Table III, together with the parameters (b_0, m, Ω) of the proposed model, computed using (10) and (11). The parameters of the first three rows of Table III were originally reported in [6], while the fourth row is taken from [42]. Loo's parameters for light, average, and heavy shadowing conditions, listed in the first, second, and the fourth rows of Table III, have been used in several studies such as [35] [42]-[45], for system simulation, analysis, and performance prediction purposes. As we expect from the theory, *m* values in Table III decrease as the amount of shadowing increases from light to average, and then to heavy. This empirical observation verifies the key role of the Nakagami *m* parameter in our model, discussed at the beginning of Section II, in modeling different types of shadow fading conditions.

In Fig. 1 we have reproduced Fig. 1 of Loo's original paper [6], using the parameters of the first three rows of Table III. The experimental data points of this figure have also been used by others [7] [9] to verify their models. In Fig. 1 we have plotted the envelope complementary CDFs (CCDFs), $\int_r^\infty p_R(x)\ dx$, for Loo's PDF and our PDF, together with the empirical data points. Interestingly, all of Loo's curves and our curves are almost indistinguishable and both are close enough to the measured data, for different cases and channel conditions. These empirical results indicate the utility of our model for LMS channels. Also note the usefulness of the parameter transformation rules given in (10) and (11), which gives almost perfect match between Loo's CCDFs and ours. The CCDFs for average shadowing in the fourth row of Table III are not included in Fig. 1, to leave the other curves readable. However, as demonstrated in Fig. 2 of our previous paper [46], Loo's model and ours perfectly match for this case as well.

As shown in Table II, Loo's model is also incorporated in the structure of several mixture models, including the Barts-Stutzman model [17] and the model of Karasawa et al. [18]. These models can be significantly simplified if we replace Loo's model with the new model. In Figs. 1, 2, and 6 of [17], four set of parameters $(\bar{K}[\text{dB}], \mu[\text{dB}], \sigma[\text{dB}])$ are given, measured in the United States at different frequency bands and elevation angles. The corresponding Loo's parameters are listed in Table IV, computed according to $b_0 = \frac{1}{2} 10^{-\bar{K}[\text{dB}]/10}$, $\mu = \frac{\ln 10}{20} \mu[\text{dB}]$, and $\sqrt{d_0} = \frac{\ln 10}{20} \sigma[\text{dB}]$. On the other hand, based on the experiments conducted in Japan, one set of parameters $(P_{r,B}[\text{dB}], m[\text{dB}], \sigma[\text{dB}])$ is given in Table I of [18], where $b_0 = \frac{1}{2} 10^{P_{r,B}[\text{dB}]/10}$, $\mu = \frac{\ln 10}{20} m[\text{dB}]$, and $\sqrt{d_0} = \frac{\ln 10}{20} \sigma[\text{dB}]$. These values are listed in Table IV as well. Corresponding to all these Loo's parameters, the parameters $(m, \ \Omega)$ of the new model are calculated using (10) and (11). Based on the parameters of Table IV, in Fig. 2 we have plotted the envelope CCDFs for Loo's model and our model. The close agreement between the two models, which is depicted in Fig. 2 over a wide range of signal levels, for several different sets of data collected at different places, frequency bands, and elevation angles, is excellent. This strongly supports the application of the proposed model for LMS channels, as a simple alternative to Loo's model. Again we draw the attention of the readers to the key role of the parameter mapping rules in (10) and (11), which allow us to conveniently use the experimental results published in the literature, to calculate the parameters of the new model.

As discussed in [7], a LMS channel model should be applicable for a wide range of elevation angles, under which the satellite is observed. One way of incorporating the effect of the elevation angle in a statistical LMS channel model is to derive empirical expressions for the parameters of the envelope PDF in terms of the elevation angle [7]. To demonstrate this procedure for our model, we have considered the experimental data published in [47], also used in [7], and have derived the following relationships by fitting polynomials over the range $20^\circ < \theta < 80^\circ$

$$b_0(\theta) = -4.7943\times10^{-8}\theta^3 + 5.5784\times10^{-6}\theta^2 - 2.1344\times10^{-4}\theta + 3.2710\times10^{-2},$$

$$m(\theta) = 6.3739\times10^{-5}\theta^3 + 5.8533\times10^{-4}\theta^2 - 1.5973\times10^{-1}\theta \;\; + 3.5156,$$

$$\Omega(\theta) = 1.4428\times10^{-5}\theta^3 - 2.3798\times10^{-3}\theta^2 + 1.2702\times10^{-1}\theta - 1.4864. \qquad (19)$$

The proposed PDF in (3), in conjunction with the above equations, compose a hybrid statistical/empirical model. The empirical and the theoretical CCDFs of the new model are plotted in Fig. 3 for different elevation angles.

B. Second-order statistics

Now we compare the LCR and the AFD of the new model with the published data in [6], assuming a slowly varying LOS, i.e., $\chi = 0$. Since the data of [6] are taken by a single antenna, we use (15) for calculating the LCR of the new model. The AFD can be obtained by dividing the integral of (3) by the LCR. To calculate the LCR, we need a model for $C_{\Re}(\tau)$, the autocovariance of the complex envelope $\Re(t)$. The spectral moments, then, can be computed according to $b_n = j^{-n} C_{\Re}^{(n)}(0)$. In this paper we consider the non-isotropic scattering correlation model $C_{\Re}(\tau) = b_0 I_0([\kappa^2 - 4\pi^2 f_{\max}^{\text{scatter}^2} \tau^2 + j4\pi\kappa\cos(\bar{\phi}) f_{\max}^{\text{scatter}} \tau]^{1/2}) / I_0(\kappa)$, where $\bar{\phi} \in [-\pi, \pi)$ is the mean direction of the angle of arrival (AOA) in the horizontal plane and $\kappa \geq 0$ is the width control parameter of the AOA [48]. This correlation model is a natural generalization of the Clarke's isotropic scattering model [48]. In fact, for $\kappa = 0$, $C_{\Re}(\tau)$ reduces to $b_0 J_0(2\pi f_{\max}^{\text{scatter}} \tau)$, a common correlation model for satellite channels [49], where $J_0(.)$ is the zero-order Bessel function of the first kind. It is easy to verify that $b_1 = b_0 2\pi f_{\max}^{\text{scatter}} \cos(\bar{\phi}) I_1(\kappa) / I_0(\kappa)$ and $b_2 = b_0 2\pi^2 f_{\max}^{\text{scatter}^2} [I_0(\kappa) + \cos(2\bar{\phi}) I_2(\kappa)] / I_0(\kappa)$.

To compare the LCR of the new model with the data published in [6], we took the parameters (b_0, m, Ω) for the light and heavy shadowing conditions from Table III. By substituting the above spectral moments b_1 and b_2 into (15) and minimizing the squared error between $N_R(r_{th}) / f_{\max}^{\text{scatter}}$ and the empirical normalized LCR data points of [6], we then obtained estimates of $\bar{\phi}$ and κ for both cases, i.e., $(\bar{\phi}, \kappa) = (1.55, 9.96)$ for light shadowing and $(\bar{\phi}, \kappa) = (1.55, 24.2)$ for heavy shadowing. As shown in Fig. 4, the LCR of the proposed model is close enough to the measured data. Using the parameters $(b_0,\ \mu,\ d_0)$ from Table III and the same $(\bar{\phi}, \kappa)$ as above, the LCR of Loo's model in (17) is also plotted in Fig. 4 for both light and heavy shadowing conditions. Similar to the very close match between the CCDFs of the two models in Fig. 1, the LCR of both models are nearly identical. As expected, we have the same situation for the AFD of both models in Fig. 5. Therefore, the parameter mapping rules given in (10) and (11) work well for the second-order statistics, as well as the first-order statistics.

To observe the utility and flexibility of the proposed model in LMS system analysis, we refer the readers to [46], [50], and [51], where three types of system performance evaluation are studied in detail: BER calculation of uncoded and coded modulations with diversity reception, interference analysis of LMS systems, and the LCR after diversity combining.

V. CONCLUSION

In this paper a new Rice-based model is proposed for land mobile satellite channels, in which the amplitude of the line-of-sight is assumed to follow the Nakagami model. We have shown that this new model has nice mathematical properties, its first- and second-order statistics can be expressed in exact closed forms, and is very flexible for data fitting, performance evaluation of narrowband and wideband land mobile satellite systems, etc.. Moreover, we have demonstrated that the proposed model fits very well to the published data in the literature, collected at different locations and frequency bands. A connection is also established between the parameters of the proposed model and those of the Loo's model, a model widely used for satellite channels. Based on this connection, the parameters of the new model can be easily derived from the estimated parameters of Loo's model, reported in the literature. This obviates the task of parameter estimation for the new model in cases where estimated Loo's parameters are available. We have also shown that the parameters of the proposed model can be related to the elevation angle. This allows the application of the model over a wide range of elevation angles.

APPENDIX

THE JOINT CF OF THE INSTANTANEOUS POWER AND ITS DERIVATIVE

Consider the narrowband stationary shadowed Rice model $\Re(t) = A(t)\exp[j\alpha(t)] + Z(t)\exp(j\zeta_0)$, with $A(t)$, $\alpha(t)$, and $Z(t)$ as independent stationary Rayleigh, uniform, and Nakagami processes. In this appendix we derive an expression for $\Phi_{S\dot{S}}(\omega_1,\omega_2)$, the joint CF of S and $\dot{S}$, defined by $E[\exp(j\omega_1 S + j\omega_2 \dot{S})]$, where $S(t) = R^2(t) = |\Re(t)|^2$ is the instantaneous power. Since the value of ζ_0 does not affect the envelope characteristics, we assume $\zeta_0 = 0$ to simplify the notation, without loss of generality. Let us define the inphase and quadrature components of $\Re(t)$ as $X(t) = A(t)\cos[\alpha(t)] + Z(t)$ and $Y(t) = A(t)\sin[\alpha(t)]$. It is easy to verify that $A(t)\cos[\alpha(t)]$ and $Y(t)$ are stationary zero mean correlated Gaussian processes, with the autocorrelation function $\mathrm{Re}[C_{\Re}(\tau)]$ and the crosscorrelation function $\mathrm{Im}[C_{\Re}(\tau)]$ [26], where Re[.] and Im[.] denote the real and imaginary parts, respectively. Clearly, the time derivative of $A(t)\cos[\alpha(t)]$ and $Y(t)$ are stationary zero mean correlated Gaussian processes as well, since differentiation is a linear operation. Hence, for a fixed instant of time t and conditioned on $Z = z$ and $\dot{Z} = \dot{z}$, the vector $\mathbf{W} = [X\ \dot{Y}\ Y\ \dot{X}]^T$, with ^{T} as the transpose operator, is a Gaussian vector with the following mean vector and covariance matrix

$$\boldsymbol{\Delta} = E[\mathbf{W} \mid Z, \dot{Z}] = \begin{bmatrix} z \\ 0 \\ 0 \\ \dot{z} \end{bmatrix}, \quad \boldsymbol{\Sigma} = \mathrm{cov}[\mathbf{W} \mid Z, \dot{Z}] = \begin{bmatrix} b_0 & b_1 & 0 & 0 \\ b_1 & b_2 & 0 & 0 \\ 0 & 0 & b_0 & -b_1 \\ 0 & 0 & -b_1 & b_2 \end{bmatrix}. \tag{A.1}$$

The elements of the covariance matrix are taken from Appendix II of [41]. Let us define $\mathbf{Q}$ as

$$\mathbf{Q} = \begin{bmatrix} \omega_1 & 0 & 0 & \omega_2 \\ 0 & 0 & \omega_2 & 0 \\ 0 & \omega_2 & \omega_1 & 0 \\ \omega_2 & 0 & 0 & 0 \end{bmatrix}. \tag{A.2}$$

Based on the identities $S = X^2 + Y^2$ and $\dot{S} = 2X\dot{X} + 2Y\dot{Y}$, it is easy to verify that $\Phi_{S\dot{S}}(\omega_1, \omega_2 \mid Z, \dot{Z}) = E[\exp(j\omega_1 S + j\omega_2 \dot{S}) \mid Z, \dot{Z}] = E[\exp(j\mathbf{W}^T\mathbf{Q}\mathbf{W}) \mid Z, \dot{Z}]$. Since conditioned on $Z = z$ and $\dot{Z} = \dot{z}$, the scalar variable $\mathbf{W}^T\mathbf{Q}\mathbf{W}$ is a quadratic form of Gaussian variables, we can use the result given in [52] to calculate its characteristic function $E[\exp(j\omega\mathbf{W}^T\mathbf{Q}\mathbf{W}) \mid Z, \dot{Z}]$ as

$$E[\exp(j\omega\mathbf{W}^T\mathbf{Q}\mathbf{W}) \mid Z, \dot{Z}] = \frac{\exp(-\boldsymbol{\Delta}^T\boldsymbol{\Sigma}^{-1}[\mathbf{I} - (\mathbf{I} - j2\omega\boldsymbol{\Sigma}\mathbf{Q})^{-1}]\boldsymbol{\Delta}/2)}{\sqrt{\det(\mathbf{I} - j2\omega\boldsymbol{\Sigma}\mathbf{Q})}}, \tag{A.3}$$

where det(.) is the determinant and $\mathbf{I}$ is the identity matrix. For $\omega = 1$ and by substituting $\boldsymbol{\Delta}$ and $\boldsymbol{\Sigma}$ from (A.1) into (A.3), and after some algebraic manipulations we obtain

$$\Phi_{S\dot{S}}(\omega_1, \omega_2 \mid Z, \dot{Z}) = \frac{1}{\vartheta}\exp\left(-\frac{(2b_2\omega_2^2 - j\omega_1)z^2 - j2\omega_2 z\dot{z} + 2b_0\omega_2^2\dot{z}^2}{\vartheta}\right), \tag{A.4}$$

where $\vartheta = 1 + 4(b_0 b_2 - b_1^2)\omega_2^2 - j2b_0\omega_1$. As demonstrated in [40], Z and $\dot{Z}$ are independent variables. The Nakagami PDF of Z is given in (1). For the Gaussian PDF of $\dot{Z}$ we have $p_{\dot{Z}}(\dot{z}) = (2\pi\sigma_{\dot{Z}}^2)^{-1/2}\exp[-\dot{z}^2/(2\sigma_{\dot{Z}}^2)]$, where $\sigma_{\dot{Z}}^2 = \chi\Omega/(4m)$, with $\chi = E[\dot{I}^2(t)]$ such that $I(t) = Z^2(t)$. By averaging $\Phi_{S\dot{S}}(\omega_1, \omega_2 \mid Z, \dot{Z})$ in (A.4) with respect to Z and $\dot{Z}$, we eventually obtain (13).

ACKNOWLEDGMENT

The work of the first, the third, and the fourth authors have been supported in part by the National Science Foundation, under the Wireless Initiative Program, Grant #9979443. The authors appreciate the input provided by Mr. C. Loo at Communications Research Center, Ottawa, ON, Canada, with regard to reproducing the empirical curves in Fig. 1.

REFERENCES

[1] W. W. Wu, “Satellite communications,” *Proc. IEEE*, vol. 85, pp. 998-1010, 1997.

[2] J. V. Evans, “Satellite systems for personal communications,” *Proc. IEEE*, vol. 86, pp. 1325-1341, 1998.

[3] B. Belloul, S. R. Saunders, M. A. N. Parks, and B. G. Evans, “Measurements and modelling of wideband propagation at L- and S-bands applicable to the LMS channel,” *IEE Proc. Microw. Antennas Propag.*, vol. 147, pp. 116-121, 2000.

[4] F. P. Fontan, M. A. V. Castro, J. Kunisch, J. Pamp, E. Zollinger, S. Buonomo, P. Baptista, and B. Arbesser, “A versatile framework for a narrow-and wide-band statistical propagation model for the LMS channel,” *IEEE Trans. Broadcasting*, vol. 43, pp. 431-458, 1997.

[5] B. Vucetic, “Propagation,” in *Satellite Communications-Mobile and Fixed Services*. M. J. Miller, B. Vucetic, and L. Berry, Eds., Boston, MA: Kluwer, 1993, pp. 57-101.

[6] C. Loo, “A statistical model for a land mobile satellite link,” *IEEE Trans. Vehic. Technol.*, vol. 34, pp. 122-127, 1985.

[7] G. E. Corazza and F. Vatalaro, “A statistical model for land mobile satellite channels and its application to nongeostationary orbit systems,” *IEEE Trans. Vehic. Technol.*, vol. 43, pp. 738-742, 1994.

[8] F. Vatalaro, “Generalized Rice-lognormal channel model for wireless communications,” *Electron. Lett.*, vol. 31, pp. 1899-1900, 1995.

[9] S. H. Hwang, K. J. Kim, J. Y. Ahn, and K. C. Whang, “A channel model for nongeostationary orbiting satellite system,” in *Proc. IEEE Vehic. Technol. Conf.*, Phoenix, AZ, 1997, pp. 41-45.

[10] T. T. Tjhung and C. C. Chai, “Fade statistics in Nakagami-lognormal channels,” *IEEE Trans. Commun.*, vol.47, pp. 1769-1772, 1999.

[11] A. Mehrnia and H. Hashemi, “Mobile satellite propagation channel: Part I - a comparative evaluation of current models,” in *Proc. IEEE Vehic. Technol. Conf.*, Amsterdam, the Netherlands, 1999, pp. 2775-2779.

[12] Y. Xie and Y. Fang, “A general statistical channel model for mobile satellite systems,” *IEEE Trans. Vehic. Technol.*, vol. 49, pp. 744-752, 2000.

[13] M. Patzold, Y. Li, and F. Laue, “A study of a land mobile satellite channel model with asymmetrical Doppler power spectrum and lognormally distributed line-of-sight component,” *IEEE Trans. Vehic. Technol.*, vol. 47, pp. 297-310, 1998.

[14] M. Patzold, U. Killat, and F. Laue, “An extended Suzuki model for land mobile satellite channels and its statistical properties,” *IEEE Trans. Vehic. Technol.*, vol. 47, pp. 617-630, 1998.

[15] G. E. Corazza, A. Jahn, E. Lutz, and F. Vatalaro, “Channel characterization for mobile satellite communications,” in *Proc. European Workshop Mobile/Personal Satcoms*, Frascati, Italy, 1994, pp. 225-250.

[16] E. Lutz, D. Cygan, M. Dippold, F. Dolainsky, and W. Papke, “The land mobile satellite communication channel –

Recording, statistics, and channel model," *IEEE Trans. Vehic. Technol.*, vol. 40, pp. 375-386, 1991.

[17] R. M. Barts and W. L. Stutzman, "Modeling and simulation of mobile satellite propagation," *IEEE Trans. Antennas Propagat.*, vol. 40, pp. 375-382, 1992.

[18] Y. Karasawa, K. Kimura, and K. Minamisono, "Analysis of availability improvement in LMSS by means of satellite diversity based on three-state propagation channel model," *IEEE Trans. Vehic. Technol.*, vol. 46, pp. 1047-1056, 1997.

[19] F. P. Fontan, J. P. Gonzalez, M. J. S. Ferreiro, A. V. Castro, S. Buonomo, and J. P. Baptista, "Complex envelope three-state Markov model based simulator for the narrow-band LMS channel," *Int. J. Sat. Commun.*, vol.15, pp.1-15, 1997.

[20] M. Rice and B. Humpherys, "Statistical models for the ACTS *K*-band land mobile satellite channel," in *Proc. IEEE Vehic. Technol. Conf.*, Phoenix, AZ, 1997, pp. 46-50.

[21] A. Mehrnia and H. Hashemi, "Mobile satellite propagation channel: Part II - a new model and its performance," in *Proc. IEEE Vehic. Technol. Conf.*, Amsterdam, the Netherlands, 1999, pp. 2780-2783.

[22] B. Vucetic and J. Du, "Channel modeling and simulation in satellite mobile communication systems," *IEEE J. Select. Areas Commun.*, vol. 10, pp. 1209-1218, 1992.

[23] F. P. Fontan, M. A. V. Castro, S. Buonomo, J. P. P. Baptista, and B. A. Rastburg, "S-band LMS propagation channel behavior for different environments, degrees of shadowing and elevation angles," *IEEE Trans. Broadcasting*, vol. 44, pp. 40-76, 1998.

[24] C. Loo and J. S. Butterworth, "Land mobile satellite channel measurements and modeling," *Proc. IEEE*, vol. 86, pp. 1442-1463, 1998.

[25] A. Abdi, H. Allen Barger, and M. Kaveh, "A simple alternative to the lognormal model of shadow fading in terrestrial and satellite channels," in *Proc. IEEE Vehic. Technol. Conf.*, Atlantic City, NJ, 2001, pp. 2058-2062.

[26] G. L. Stuber, *Principles of Mobile Communication*. Boston, MA: Kluwer, 1996.

[27] I. S. Gradshteyn and I. M. Ryzhik, *Table of Integrals, Series, and Products*, 5th ed., A. Jeffrey, Ed., San Diego, CA: Academic, 1994.

[28] W. Magnus, F. Oberhettinger, and R. P. Soni, *Formulas and Theorems for the Special Functions of Mathematical Physics*, 3rd ed., New York: Springer, 1966.

[29] J. Abad and J. Sesma, "Computation of the regular confluent hypergeometric function," *The Mathematica J.*, vol. 5, no. 4, pp. 74-76, 1995.

[30] V. A. Melititskiy, V. L. Rumyantsev, and N. S. Akinshin, "Estimate of the average power of signals with an *m*-distribution in the presence of normal interference," *Soviet J. Commun. Technol. Electron.*, vol. 33, no. 5, pp. 130-132, 1988.

[31] F. McNolty, "Applications of Bessel function distributions," *Sankhyā : Ind. J. Statist. B*, vol. 29, pp. 235-248, 1967.

[32] V. A. Melititskiy, N. S. Akinshin, V. V. Melititskaya, and A. V. Mikhailov, "Statistical characteristics of a non-Gaussian signal envelope in non-Gaussian noise," *Telecommun. Radio Eng., pt. 2-Radio Eng*, vol. 41, no. 11, pp. 125-129, 1986.

[33] S. K. Bhattacharya, "Confluent hypergeometric distributions of discrete and continuous type with applications to accident proneness," *Calcutta Statist. Assoc. Bull.*, vol. 15, no. 57, pp. 20-31, 1966.

[34] M. K. Simon and M. S. Alouini, *Digital Communication over Fading Channels: A Unified Approach to Performance Analysis*. New York: Wiley, 2000.

[35] S. H. Jamali and T. L. Ngoc, *Coded-Modulation Techniques for Fading Channels*. Boston, MA: Kluwer, 1994.

[36] J. M. Morris and J. L. Chang, “Burst error statistics of simulated Viterbi decoded BFSK and high-rate punctured codes on fading and scintillating channels,” *IEEE Trans. Commun.*, vol. 43, pp. 695-700, 1995.

[37] A. J. Goldsmith and S. G. Chua, "Variable-rate coded M-QAM for fading channels", *IEEE Trans. Commun.*, vol. 45, pp. 1218-1230, 1997.

[38] L. F. Chang, “Throughput estimation of ARQ protocols for a Rayleigh fading channel using fade- and interfade-duration statistics,” *IEEE Trans. Vehic. Technol.*, vol. 40, pp. 223-229, 1991.

[39] A. Abdi and M. Kaveh, “Level crossing rate in terms of the characteristic function: A new approach for calculating the fading rate in diversity systems,” accepted for publication in *IEEE Trans. Commun.*.

[40] N. Youssef, T. Munakata, and M. Takeda, “Fade statistics in Nakagami fading environments,” in *Proc. IEEE Int. Symp. Spread Spectrum Techniques Applications*, Mainz, Germany, 1996, pp. 1244-1247.

[41] S. O. Rice, "Statistical properties of a sine wave plus random noise," *Bell Syst. Tech. J.*, vol. 27, pp. 109-157, 1948.

[42] C. Loo, “Digital transmission through a land mobile satellite channel,” *IEEE Trans. Commun.*, vol. 38, pp. 693-697, 1990.

[43] C. Loo and N. Secord, “Computer models for fading channels with applications to digital transmission,” *IEEE Trans. Vehic. Technol.*, vol. 40, pp. 700-707, 1991.

[44] Y. A, Chau and J. T. Sun, “Diversity with distributed decisions combining for direct-sequence CDMA in a shadowed Rician-fading land-mobile satellite channel,” *IEEE Trans. Vehic. Technol.*, vol. 45, pp. 237-247, 1996.

[45] R. D. J. van Nee and R. Prasad, “Spread spectrum path diversity in a shadowed Rician fading land-mobile satellite channel,” *IEEE Trans. Vehic. Technol.*, vol. 42, pp. 131-136, 1993.

[46] A. Abdi, W. C. Lau, M.-S. Alouini, and M. Kaveh, “A new simple model for land mobile satellite channels,” in *Proc. IEEE Int. Conf. Commun.*, Helsinki, Finland, 2001, pp. 2630-2634.

[47] M. Sforza and S. Buonomo, “Characterization of the LMS propagation channel at L- and S-bands: Narrowband experimental data and channel modeling,” in *Proc. NASA Propagation Experiments (NAPEX) Meeting and the Advanced Communications Technology Satellite (ACTS) Propagation Studies Miniworkshop*, Pasadena, CA, 1993, pp. 183-192.

[48] A. Abdi, H. Allen Barger, and M. Kaveh, “A parametric model for the distribution of the angle of arrival and the associated correlation function and power spectrum at the mobile station,” accepted for publication in *IEEE Trans. Vehic. Technol.*.

[49] F. Vatalaro and F. Mazzenga, “Statistical channel modeling and performance evaluation in satellite personal communications,” *Int. J. Satell. Commun.*, vol. 16, pp. 249-255, 1998.

[50] A. Abdi, W. C. Lau, M.-S. Alouini, and M. Kaveh, “On the second-order statistics of a new simple model for land mobile satellite channels,” in *Proc. IEEE Vehic. Technol. Conf.*, Atlantic City, NJ, 2001, pp. 301-304.

[51] A. Abdi, “Modeling and estimation of wireless fading channels with applications to array-based communication,” Ph.D. Thesis, Dept. of Elec. and Comp. Eng., University of Minnesota, Minneapolis, MN, 2001.

[52] G. L. Turin, “The characteristic function of Hermitian quadratic forms in complex normal variables,” *Biometrika*, vol. 47, pp. 199-201, 1960.

FIGURE CAPTIONS

Fig. 1. Complementary cumulative distribution function of the signal envelope in a land mobile satellite channel in Canada, under different shadowing conditions: Measured data [6], Loo's model [6], and the proposed model.

Fig. 2. Complementary cumulative distribution function of the signal envelope in different land mobile satellite channels in the United States and Japan: Loo's model [17] [18] and the proposed model.

Fig. 3. Complementary cumulative distribution function of the signal envelope in a land mobile satellite channel for different elevation angles: Measured data [47] and the proposed model.

Fig. 4. Level crossing rate of the signal envelope in a land mobile satellite channel with light and heavy shadowing: Measured data [6], Loo's model [13], and the proposed model (see Table III for the parameter values).

Fig. 5. Average fade duration of the signal envelope in a land mobile satellite channel with light and heavy shadowing: Measured data [6], Loo's model [13], and the proposed model (see Table III for the parameter values).

TABLE CAPTIONS

Table I. A List of the Proposed Single Models for Narrowband Satellite Channels

Table II. A List of the Proposed Mixture Models for Narrowband Satellite Channels

Table III. Loo's Parameters [6] [42] and the Corresponding Parameters of the New Model, Calculated from (10) and (11)

Table IV. Loo's Parameters [17] [18] and the Corresponding Parameters of the New Model, Calculated from (10) and (11)

Table I A LIST OF THE PROPOSED SINGLE MODELS FOR NARROWBAND SATELLITE CHANNELS

Proposed by	Year	Multipath fading	LOS shadow fading	Multiplicative shadow fading	Comments
Loo [6]	1985	Rice	lognormal	---	---
Corazza-Vatalaro [7]	1994	Rice	---	lognormal	---
Vatalaro [8]	1995	Rice	---	lognormal	includes an extra additive scatter component.
Hwang et al. [9]	1997	Rice	lognormal	---	the power of the scatter components is random.
Tjhung-Chai [10]	1999	Nakagami	---	lognormal	---
Mehrnia-Hashemi [11]	1999	Nakagami	---	---	---
Mehrnia-Hashemi [11]	1999	Norton	---	---	---
Xie-Fang [12]	2000	Beckmann	---	lognormal	---

Table II A LIST OF THE PROPOSED MIXTURE MODELS FOR NARROWBAND SATELLITE CHANNELS

Proposed by	Year	Structure of the model
Lutz et al. [16]	1991	Rice+Suzuki
Barts-Stutzman [17]	1992	Rice+Loo
Karasawa et al [18]	1997	Rice+Loo+Rayleigh
Fontan et al. [19]	1997	Loo+Loo+Loo
Rice-Humpherys [20]	1997	Rice+Rice+Suzuki
Mehrnia-Hashemi [21]	1999	Rice+Hoyt

Table III LOO'S PARAMETERS [6] [42] AND THE CORRESPONDING PARAMETERS OF THE NEW MODEL, CALCULATED FROM (10) AND (11)

	Loo's model			The new model	
	μ	$\sqrt{d_0}$	b_0	m	Ω
Infrequent light shadowing	0.115	0.115	0.158	19.4	1.29
Frequent heavy shadowing	-3.914	0.806	0.063	0.739	8.97×10^{-4}
Overall results	-0.690	0.230	0.251	5.21	0.278
Average shadowing	-0.115	0.161	0.126	10.1	0.835

Table IV LOO'S PARAMETERS [17] [18] AND THE CORRESPONDING PARAMETERS OF THE NEW MODEL, CALCULATED FROM (10) AND (11)

		Loo's model			The new model	
	Data set no.	μ	$\sqrt{d_0}$	b_0	m	Ω
Data sets of Barts and Stutzman [17]	1	-0.341	0.099	0.005	26	0.515
	2	-0.528	0.187	0.0129	7.64	0.372
	3	-0.935	0.128	3.97×10^{-3}	15.8	0.159
	4	-1.092	0.15	0.0126	11.6	0.118
Data set of Karasawa et al. [18]	5	-1.15	0.345	0.0158	2.56	0.123

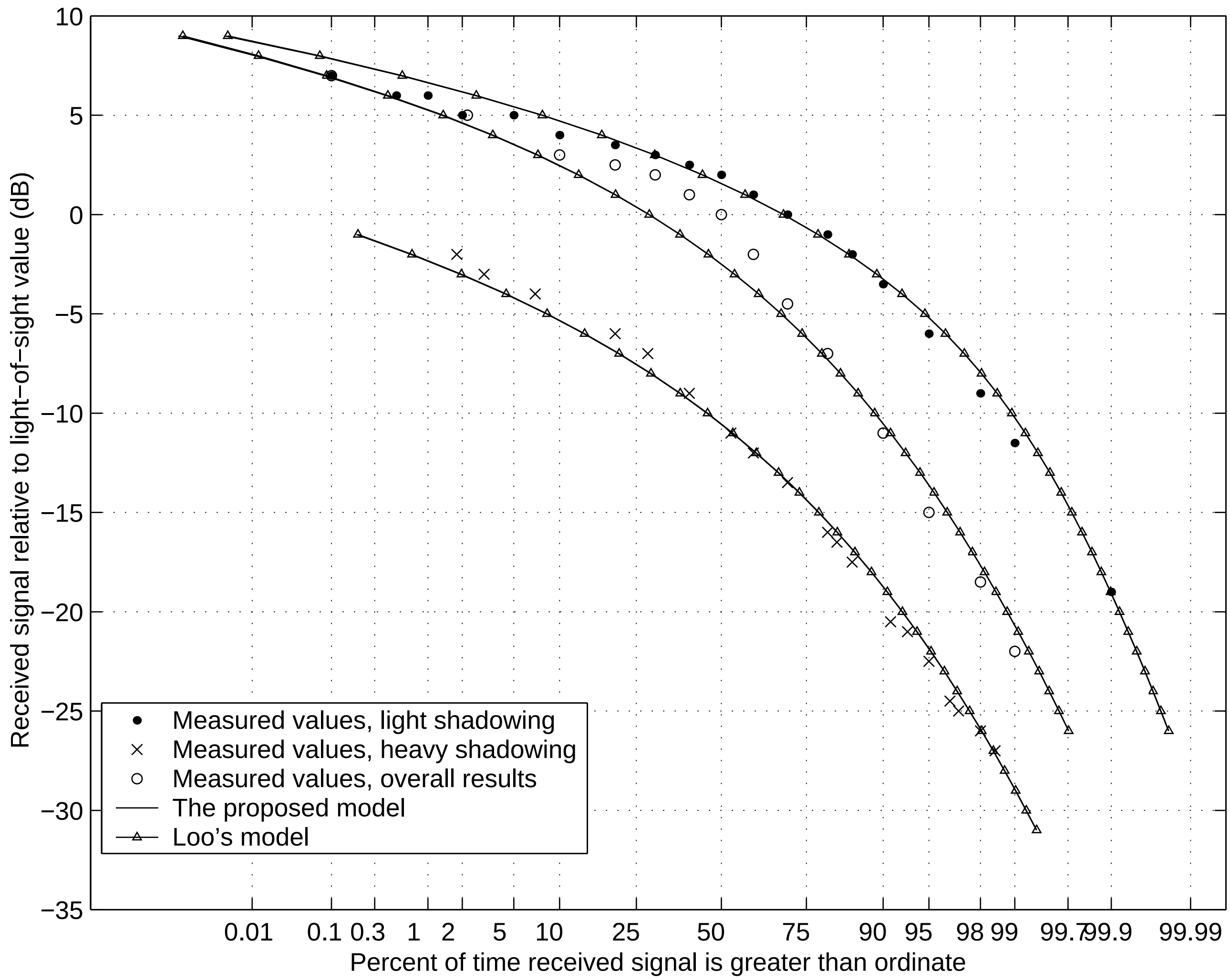

Fig. 1. Complementary cumulative distribution function of the signal envelope in a land mobile satellite channel in Canada, under different shadowing conditions: Measured data [6], Loo's model [6], and the proposed model.

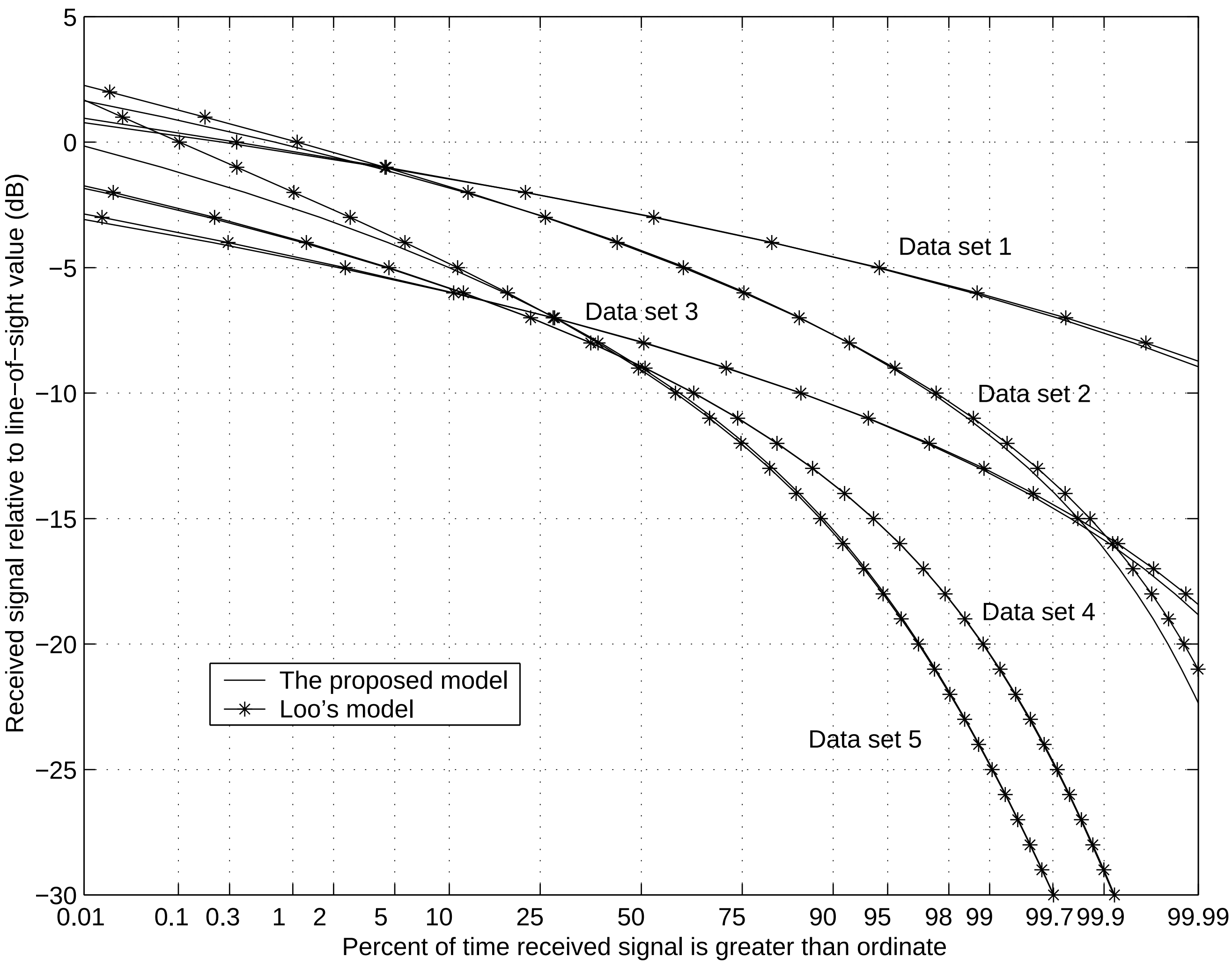

Fig. 2. Complementary cumulative distribution function of the signal envelope in different land mobile satellite channels in the United States and Japan: Loo's model [17] [18] and the proposed model.

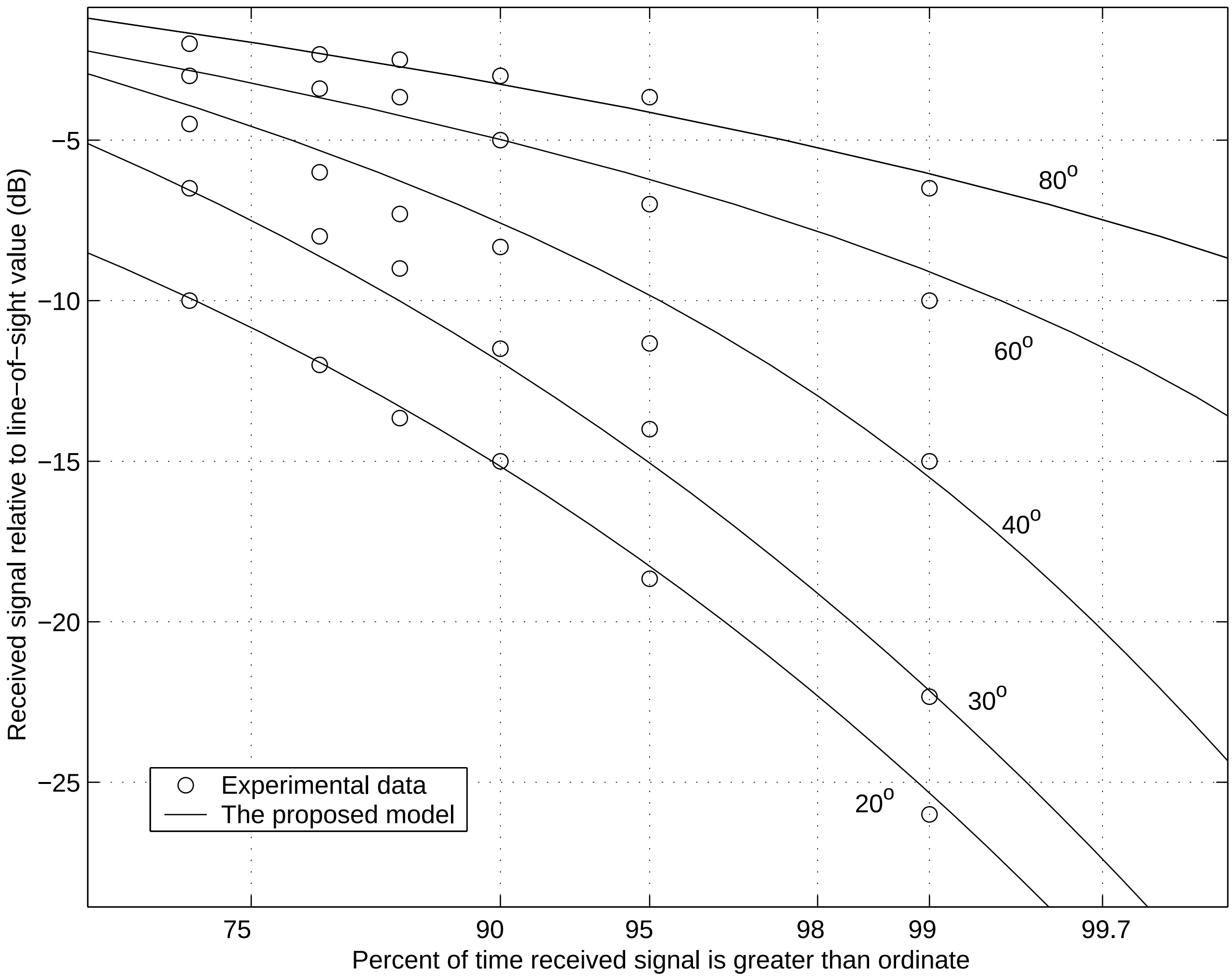

Fig. 3. Complementary cumulative distribution function of the signal envelope in a land mobile satellite channel for different elevation angles: Measured data [47] and the proposed model.

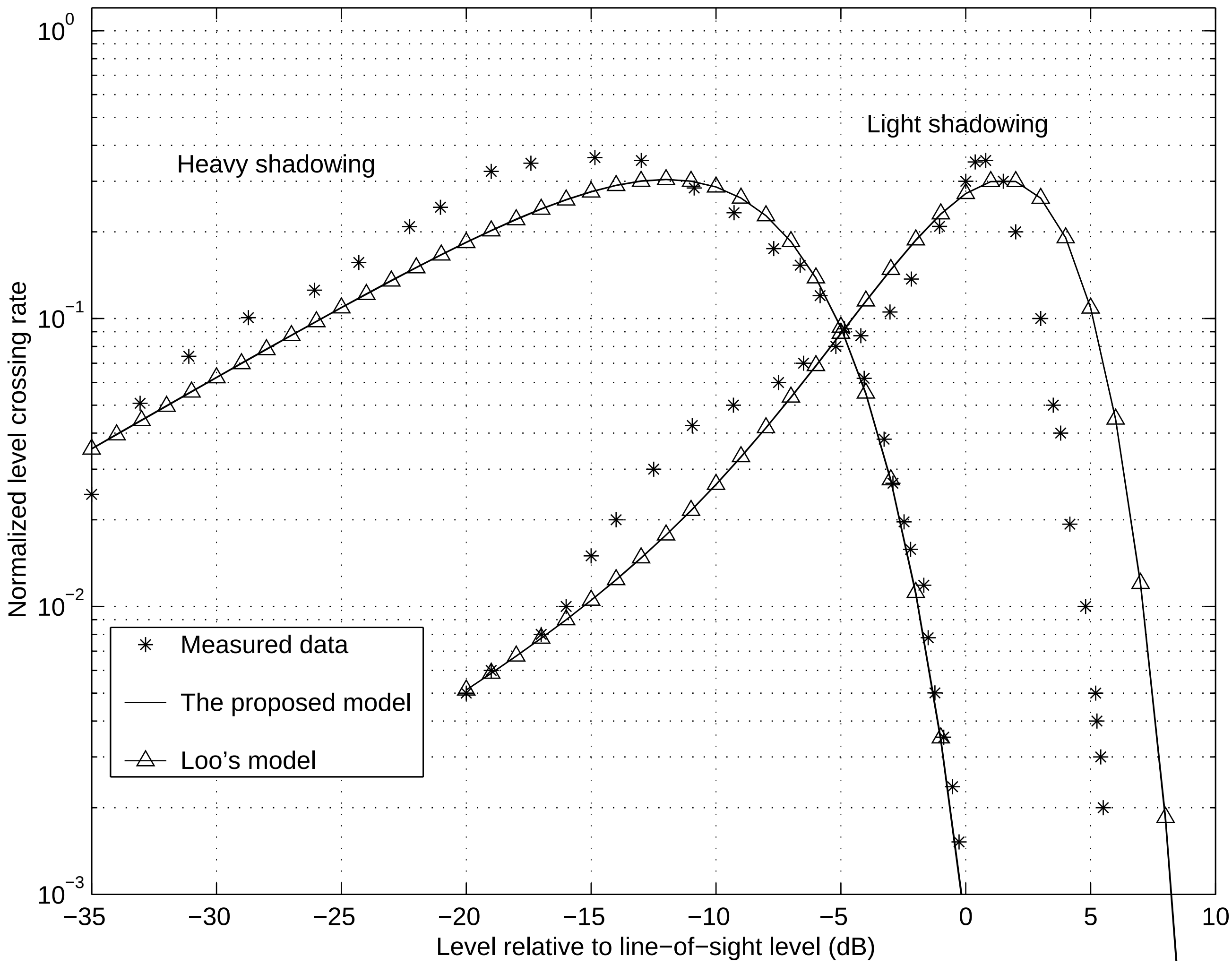

Fig. 4. Level crossing rate of the signal envelope in a land mobile satellite channel with light and heavy shadowing: Measured data [6], Loo's model [13], and the proposed model (see Table III for the parameter values).

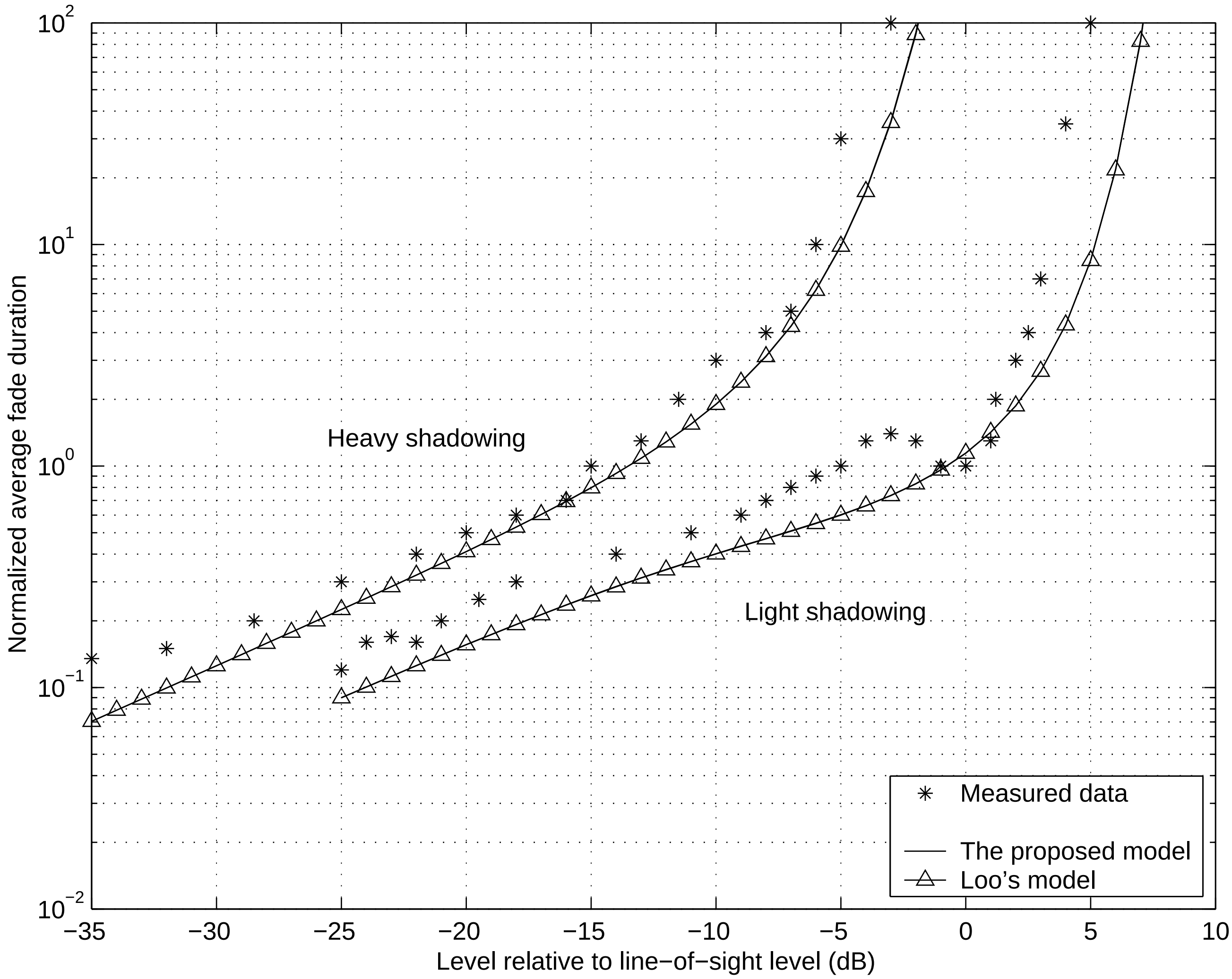

Fig. 5. Average fade duration of the signal envelope in a land mobile satellite channel with light and heavy shadowing: Measured data [6], Loo's model [13], and the proposed model (see Table III for the parameter values).